AMERICAN SOCIETY FOR MICROBIOLOGY | mBio®

RESEARCH ARTICLE

Ssn6 Defines a New Level of Regulation of White-Opaque Switching in *Candida albicans* and Is Required For the Stochasticity of the Switch

Aaron D. Hernday,[a] Matthew B. Lohse,[b*] Clarissa J. Nobile,[a,b] Liron Noiman,[b,c] Clement N. Laksana,[a] Alexander D. Johnson[b,d]

Department of Molecular and Cell Biology, School of Natural Sciences, University of California, Merced, Merced, California, USA[a]; Department of Microbiology and Immunology,[b] Tetrad Program, Department of Biochemistry and Biophysics,[c] and Department of Biochemistry and Biophysics,[d] University of California, San Francisco, San Francisco, California, USA

* Present address: Matthew B. Lohse, Department of Biology, BioSynesis, Inc., San Francisco, California, USA.

A.D.H., M.B.L., and C.J.N. contributed equally to this work.

ABSTRACT **The human commensal and opportunistic pathogen *Candida albicans* can switch between two distinct, heritable cell types, named "white" and "opaque," which differ in morphology, mating abilities, and metabolic preferences and in their interactions with the host immune system. Previous studies revealed a highly interconnected group of transcriptional regulators that control switching between the two cell types. Here, we identify Ssn6, the *C. albicans* functional homolog of the *Saccharomyces cerevisiae* transcriptional corepressor Cyc8, as a new regulator of white-opaque switching. In a or α mating type strains, deletion of *SSN6* results in mass switching from the white to the opaque cell type. Transcriptional profiling of *ssn6* deletion mutant strains reveals that Ssn6 represses part of the opaque cell transcriptional program in white cells and the majority of the white cell transcriptional program in opaque cells. Genome-wide chromatin immunoprecipitation experiments demonstrate that Ssn6 is tightly integrated into the opaque cell regulatory circuit and that the positions to which it is bound across the genome strongly overlap those bound by Wor1 and Wor2, previously identified regulators of white-opaque switching. This work reveals the next layer in the white-opaque transcriptional circuitry by integrating a transcriptional regulator that does not bind DNA directly but instead associates with specific combinations of DNA-bound transcriptional regulators.**

IMPORTANCE **The most common fungal pathogen of humans, *C. albicans*, undergoes several distinct morphological transitions during interactions with its host. One such transition, between cell types named "white" and "opaque," is regulated in an epigenetic manner, in the sense that changes in gene expression are heritably maintained without any modification of the primary genomic DNA sequence. Prior studies revealed a highly interconnected network of sequence-specific DNA-binding proteins that control this switch. We report the identification of Ssn6, which defines an additional layer of transcriptional regulation that is critical for this heritable switch. Ssn6 is necessary to maintain the white cell type and to properly express the opaque cell transcriptional program. Ssn6 does not bind DNA directly but rather associates with specific combinations of DNA-bound transcriptional regulators to control the switch. This work is significant because it reveals a new level of regulation of an important epigenetic switch in the predominant fungal pathogen of humans.**

Received 12 November 2015 **Accepted** 28 December 2015 **Published** 26 January 2016

Citation Hernday AD, Lohse MB, Nobile CJ, Noiman L, Laksana CN, Johnson AD. 2016. Ssn6 defines a new level of regulation of white-opaque switching in *Candida albicans* and is required for the stochasticity of the switch. mBio 7(1):e01565-15. doi:10.1128/mBio.01565-15.

Editor John W. Taylor, University of California

Address correspondence to Aaron D. Hernday, ahernday@ucmerced.edu, or Alexander D. Johnson, ajohnson@cgl.ucsf.edu.

Complex, interlocking networks of transcriptional regulators and their target genes lie at the foundation of many important cell fate choices. The white-opaque switch in the fungal species *Candida albicans* is an example that occurs in a unicellular eukaryote. As such, the white-opaque switch represents a cell fate decision amenable to extensive genetic, biochemical, and systems level dissection.

C. albicans is a part of the normal human microbiota and is also an opportunistic pathogen that can reside in many diverse niches within the human host. *C. albicans* can undergo a number of morphological changes, including the well-studied switch from the "white" to the "opaque" cell type (1–6). These two cell types are heritable for many generations (~10^4), and the switch between them occurs epigenetically, that is, without any change in the primary DNA sequence of the genome. White cells are spherical and produce shiny, domed colonies under standard laboratory conditions, while opaque cells are elongated and produce flatter, darker colonies (4) (Fig. 1). In addition to these physical distinctions, the two cell types display different mating abilities (7), metabolic preferences (8), and interactions with host immune cells (9–13). Several environmental inputs influence the frequency of switching between the

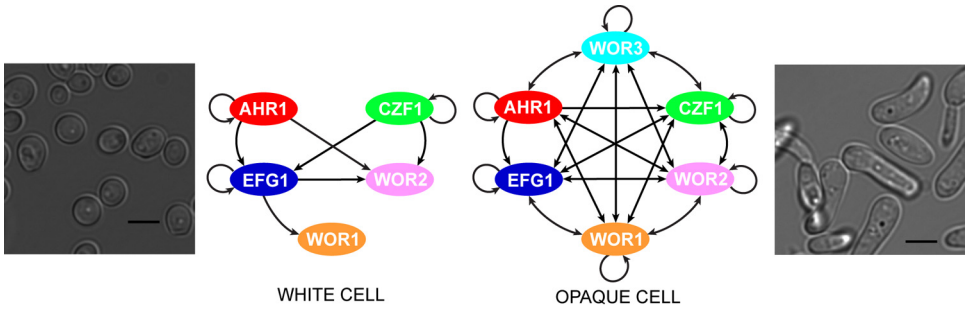

FIG 1 Working model for the white-opaque regulatory circuit. The figure shows the regulatory network in white cells (center left) and opaque cells (center right), based on previously published ChIP-chip data (17, 23, 24). Arrows represent direct binding interactions for the various transcriptional regulators. Images of typical white (far left) and opaque (far right) cells are also shown. Bar, 5 μm.

two cell types; these include temperature (14), carbon dioxide levels (15), and carbon source (16, 17).

The white-opaque switch in *C. albicans* is one of the most extensively studied epigenetic switches in any eukaryotic organism. Currently, six sequence-specific DNA binding proteins (Wor1, Wor2, Wor3, Czf1, Efg1, and Ahr1) are known to regulate the switch (17–24) (Fig. 1). Wor1, the "master regulator," is highly upregulated in opaque cells, drives mass switching to the opaque cell type when overexpressed, and, when deleted, "locks" cells in the white cell type. Under standard laboratory conditions and in standard laboratory strains, Wor1 is repressed by the a1-α2 heterodimer, and for this reason, only strains homozygous at their mating type locus are switching competent (7, 18, 19, 21). Wor2, Wor3, and Czf1 are also upregulated in opaque cells and are required to maintain the opaque cell type and permit switching at the appropriate frequency (17, 22, 23). Analogous to Wor1, but acting in the opposite direction, Efg1 is a white-cell-enriched regulator that, when overexpressed, drives switching from opaque-to-white (23–25). The recently identified regulator Ahr1, which represses the switch from white-to-opaque in an Efg1-dependent manner (20, 24), is the first identified regulator of white-opaque switching that is not differentially transcriptionally regulated between the two cell types.

In this paper, we identify Ssn6 as a core regulator of white-opaque switching. Unlike the six previously described regulators of white-opaque switching, Ssn6 does not bind DNA directly and specifically; rather, based on the behavior of its ortholog in *Saccharomyces cerevisiae*, it is recruited to DNA by sequence-specific DNA binding proteins. Our results establish that Ssn6 represents a second layer of white-opaque switching regulation, where it represses genes through association with the previously described sequence-specific regulators.

RESULTS

Deletion of *SSN6* results in cells that are locked in the opaque phenotype (opaque-locked cells). To identify additional members of the white-opaque regulatory network, we extensively analyzed the available genome-wide chromatin immunoprecipitation and transcriptional profiling data for the white-opaque regulatory circuit (17, 23, 24, 26). We found that three of the six known regulators (Wor1, Wor2, and Efg1) bind upstream of the *SSN6* gene (orf19.6798). On the basis of this evidence, we hypothesized that Ssn6 plays a role in regulating white-opaque switching.

To test the hypothesis that Ssn6 controls white-opaque switching, we converted an a/α *ssn6* deletion strain (27) to the switching-competent a/Δ and α/Δ states, where either the **a** locus or the α locus had been deleted. Normally, a/Δ and α/Δ strains switch back and forth between white and opaque cells, but the a/Δ *ssn6* and α/Δ *ssn6* deletion strains exclusively formed cells and colonies that phenotypically resembled opaque cells; we were unable to isolate any white cells (see Table S1A in the supplemental material). To confirm this result, we generated an independent *ssn6* deletion mutant strain in a "standard" switching background (an a/a strain produced by sorbose selection). Again, the a/a *ssn6* deletion strain gave rise exclusively to opaque-looking cells (Fig. 2), and several independent switching assays supported the conclusion that these strains were "locked" in the opaque cell type (Table 1).

Because mating is a hallmark of the opaque cell type of *C. albicans*, we performed quantitative mating assays with wild-type and *ssn6* deletion opaque strains to further test whether **a** or α *ssn6* deletion strains are phenotypically opaque. We observed that both a/Δ *ssn6* and α/Δ *ssn6* deletion strains (which are opaque locked) mate with efficiencies that are within 10-fold of those of wild-type

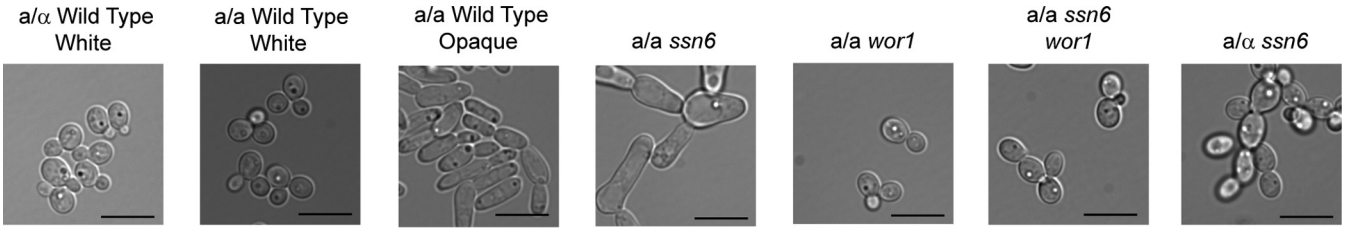

FIG 2 Single-cell morphology of strains deleted for *SSN6*. Typical cells of wild-type white and opaque strains as well as *ssn6* and *ssn6 wor1* deletion strains of the indicated mating types grown overnight at room temperature are shown. Bar, 10 μm.

TABLE 1 Ssn6 deletion strain white-to-opaque and opaque-to-white switching frequencies

Switching direction and strain	Switch frequency (%)	*n*
White-to-opaque		
a/a wild-type white	8.62	580
a/a *SSN6*/*ssn6* white	4.96	605
a/a *ssn6* white[a]	(100)	NA
a/a *ssn6 wor1* white	<0.16	629
a/a *ssn6 wor1* white	<0.15	666
a/α *ssn6* white	<0.37	273
a/a *wor1* white	<0.17	586
Opaque-to-white		
a/a wild-type opaque	5.78	450
a/a *ssn6* opaque	<0.29	350

[a] We were unable to get a white isolate of this strain and so were unable to perform the normal white-to-opaque switching assay.

opaque cells and are at least 1,000-fold higher than the efficiencies seen in mating between wild-type **a** and α white cells (see Table S2 in the supplemental material).

We note that a/a heterozygous *SSN6*/*ssn6* strains exhibited a normal white-to-opaque switch frequency (~5%; Table 1), suggesting no haploinsufficiency of Ssn6 in relation to its role in regulating white-opaque switching. Ectopic expression of *SSN6* in white cells did not prevent switching to the opaque cell type, and ectopic expression in opaque cells did not result in mass switching to the white cell type (see Table S1B in the supplemental material), results consistent with the fact that *SSN6* is not differentially regulated between the two cell types. These results are also consistent with the idea that Ssn6 is recruited to DNA by sequence-specific DNA binding proteins. In the absence of the relevant DNA-bound proteins, overexpression of *SSN6* would be expected to produce little effect.

In *S. cerevisiae*, Ssn6 (Cyc8) is tightly bound to Tup1, and the two function together as a complex. This is most clearly evidenced by the fact that *tup1* and *cyc8* deletions produce virtually the same phenotypes in *S. cerevisiae* and result in the same genes being derepressed. This is not the case in *C. albicans*. García-Sánchez et al. showed, using microarrays and deletion strains, that Ssn6 and Tup1 control different sets of genes in a/α cells (28). Park and Morschhäuser showed that a *tup1* deletion has only a modest effect, if any, on white-opaque switching (29). This is in contrast to the large effects observed here for the *ssn6* deletion. Taken together, these results indicate that, in *C. albicans*, Ssn6 functions independently of Tup1. To confirm this, we converted an a/α *tup1* deletion strain (27) to the switching-capable a/Δ background and compared it to an a/Δ *ssn6* strain. Again, the two deletions produced very different phenotypes: the *tup1* deletion is hyperfilamentous, whereas the *ssn6* deletion is not (see Fig. S1 in the supplemental material).

Wor1 is necessary for establishment of the opaque cell type in the *ssn6* deletion mutant. To date, expression of *WOR1* has always proven necessary for both the establishment and maintenance of the opaque cell type. To determine if deletion of *SSN6* could circumvent the requirement for Wor1, we constructed an a/a *ssn6 wor1* double-deletion strain. Just as for a *wor1* deletion strain, the *ssn6 wor1* double-deletion strain produced no opaque sectors or colonies (Table 1). This strain exhibited single-cell morphologies similar to those seen with the a/α *ssn6* deletion strain (which is incapable of switching to the opaque form) (Fig. 2). These results show that Wor1 remains necessary for the establishment and maintenance of the opaque cell type, even in the absence of *SSN6*; that is, *WOR1* is epistatic to *SSN6*.

Transcriptional profiling of the *ssn6* deletion mutants. We next examined the transcriptional changes produced by deleting *SSN6*. On the basis of the results seen with its ortholog in *S. cerevisiae*, we predicted that Ssn6 should function as a repressor in *C. albicans*. Consistent with this expectation, transcriptional profiling of the various deletion mutants (i.e., comparison of the a/α *ssn6*, a/a *ssn6*, and a/a *ssn6 wor1* mutants to the wild-type) revealed that the transcriptional levels of differentially regulated genes largely increased rather than decreased upon deletion of *SSN6* (see Table S3 and Data Set S1 in the supplemental material). We note that our overall array results obtained with the a/α *ssn6* deletion strain are in good agreement with the results obtained by García-Sánchez et al. using an independently derived a/α *ssn6* deletion strain (28).

A number of genes were upregulated in all three of our *ssn6* deletion mutant strains (the a/α *ssn6*/*ssn6*, a/a *ssn6*/*ssn6*, and a/a *ssn6*/*ssn6 wor1*/*wor1* strains) relative to the white or opaque parental strains. These genes, which are neither white- nor opaque-phase-enriched, appear to represent a "general" *ssn6* regulon unrelated to white-opaque switching (see Fig. S2 in the supplemental material).

Ssn6 represses the opaque cell transcriptional program in white cells. We next considered the role of Ssn6 in specifying the white and opaque cell types. We focus here on a conservative set of 41 genes that are significantly upregulated in white cells compared to opaque cells (14 genes) or vice versa (27 genes) (see Data Set S1 in the supplemental material). These genes were chosen as being white- or opaque-phase-enriched at least 3-fold in each of four different studies (24, 26, 30; this study).

Of the 27 opaque-phase-enriched genes, 26 were upregulated relative to wild-type white cells when *SSN6* was deleted from a/a cells. As described above, these cells are locked in the opaque form, so it is not surprising that the opaque-phase-enriched genes are upregulated. However, when *SSN6* was deleted from a/α cells, only 7 of these genes were upregulated compared to the wild-type a/α cell results (Fig. 3). Six of these same seven genes were upregulated when *SSN6* was deleted from *wor1* deletion strains. These results divide the opaque-phase-enriched genes into two groups: Wor1-independent genes (7 genes) and Wor1-dependent genes (20 genes). We note that we observe a similar division of opaque-enriched genes into Wor1-independent and Wor1-dependent sets when considering an expanded set of white- and opaque-phase enriched genes (see Fig. S2 in the supplemental material).

Ssn6 represses the white cell transcriptional program in opaque cells. We next considered the behavior of the 14 representative white-phase-enriched genes. When *SSN6* was deleted, most of these genes were expressed at higher levels in opaque cells (Fig. 3). In other words, Ssn6 is required to repress the white cell transcriptional program in opaque cells (this trend also held true when we analyzed an expanded set of white-phase-enriched genes). We noted that when *SSN6* was deleted in the a/a background, the resulting cell type, although an opaque cell in appearance and colony morphology, also had many white-phase-enriched genes expressed. Thus, although these cells phenotypically resemble opaque cells, their tran-

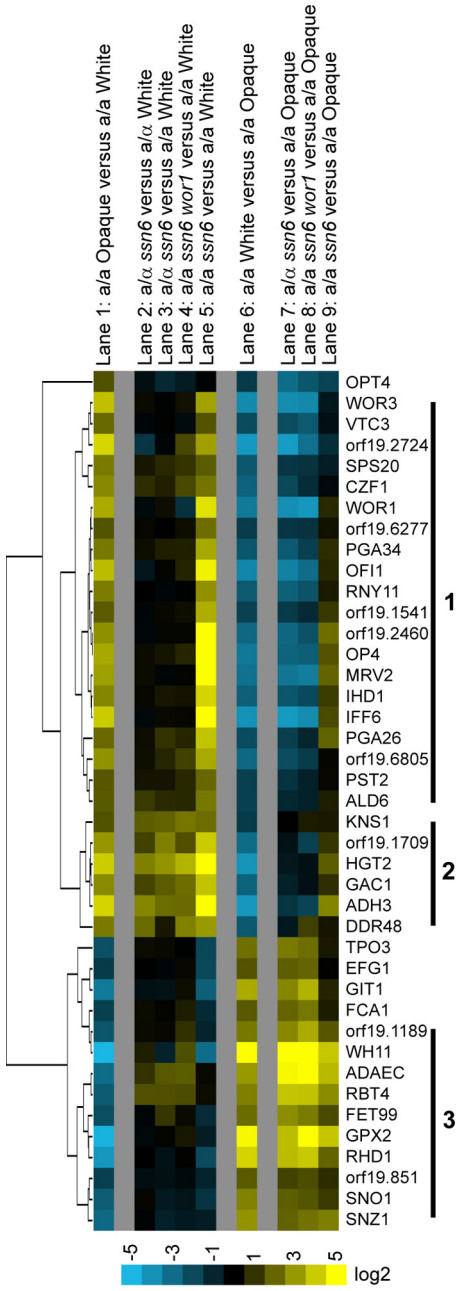

FIG 3 Microarray analysis of the *ssn6* and *ssn6 wor1* deletion strains relative to white and opaque cells for a core set of 41 white- and opaque-phase-enriched genes. Transcriptional changes in a/α (lanes 2 to 3 and 7) and a/a (lanes 5 and 9) *ssn6* deletion strains as well as the a/a *wor1 ssn6* deletion strain (lanes 4 and 8) relative to the white (lanes 2 to 5) and opaque (lanes 7 to 9) parent strains are shown. Opaque (lane 1) or white (lane 6) enrichment of these genes in the wild-type background from the same transcriptional profiling are included for comparison. Three groups of genes emerged from the cluster analysis: normally opaque-phase-enriched genes that are not upregulated in the a/α *ssn6* or the a/a *wor1 ssn6* deletion strains (group 1), opaque-phase-enriched genes that are upregulated in all of the deletion backgrounds (group 2), and white-phase-enriched genes that are not downregulated in the opaque a/a *ssn6* deletion strain (group 3). The 41 genes shown were differentially regulated at least 3-fold between white and opaque cells in this study as well as in three others (24, 26, 30).

scriptome is not identical to that of conventional opaque cells. This may explain why *SSN6* is not differentially regulated between the two cell types, since it likely plays an important role in both white and opaque cells. This may also help explain why the efficiency of mating of *ssn6* deletion cells was slightly below that of true opaque cells.

The transcriptional profile of the three *ssn6* deletion strains suggests that the behavior of significant portions of the white and opaque regulons (roughly 70% and 25%, respectively) is orchestrated through Ssn6-dependent regulation. In other words, while the cell type determination is determined by the balance between Wor1 and Efg1, large portions of both cell type programs can be expressed at the same time and Ssn6 is involved in the mutual repression of these programs according to the cell type.

Identification of "direct" targets of Ssn6 in white and opaque cells. In order to identify the direct targets of Ssn6 and to evaluate the degree to which Ssn6 is incorporated into the known white-opaque regulatory network, we performed genome-wide chromatin immunoprecipitation (ChIP-chip) experiments for Ssn6 in both white and opaque cell types.

In white cells, we identified 38 high-confidence Ssn6 binding sites corresponding to 22 intergenic regions positioned upstream of 31 genes (Fig. 4A and B; see also Fig. S3A, Data Set S1, and Data Set S2 in the supplemental material). Of these 31, 11 (6 opaque-phase-enriched and 5 white-phase-enriched genes) are differentially expressed by at least 2-fold between white and opaque cells based on our transcriptome sequencing (RNA-seq) data (26) (see Data Set S1). We examined the degree of overlap of the peaks of Ssn6 binding in white cells and those of Ahr1, Czf1, and Efg1, which are expressed in white cells (24). Roughly 40% of Ssn6-bound intergenic regions are also bound by at least one of these other three regulators (Fig. 4B; see also Data Set S3A and B). This result is consistent with the transcriptional profiling data and indicates that an important role of Ssn6 is to repress the opaque program in white cells. Consistent with the transcriptional profiling results, the Ssn6 ChIP results show that Ssn6 plays additional roles in white cells that are not directly related to white-opaque switching.

In opaque cells, Ssn6 binds to 237 high-confidence sites corresponding to 166 intergenic regions upstream of 232 genes (see Data Set S1 and S2 in the supplemental material). Of these 232 potential target genes, 107 (59 opaque-phase-enriched and 48 white-phase-enriched genes) are differentially expressed by at least 2-fold between white and opaque cells based on our RNA-seq data (26) (see Data Set S1). Strikingly, more than 99% (165 of 166) of Ssn6-bound intergenic regions are bound by at least one of the other six regulators of white-opaque switching (Wor1, Wor2, Wor3, Czf1, Efg1, and Ahr1), more than 90% of the Ssn6-bound intergenic regions are bound by either Wor1 or Wor2, and approximately 80% of these are also bound by Efg1 (Fig. 4C and D; see also Fig. S3B and C). In addition to the propensity to bind in association with Wor1 and Wor2, Ssn6 tends to be found at sites bound by multiple regulators; more than 85% of Ssn6 binding events are at locations where three or more other regulators are also bound. These trends are much greater than would be expected by chance (see Data Set S3D). The change in the distribution of Ssn6 across the genome between white and opaque cells represents a complete reconfiguration of Ssn6; it appears largely driven by the presence of Wor1, Wor2, and Efg1 in opaque cells. As might be expected

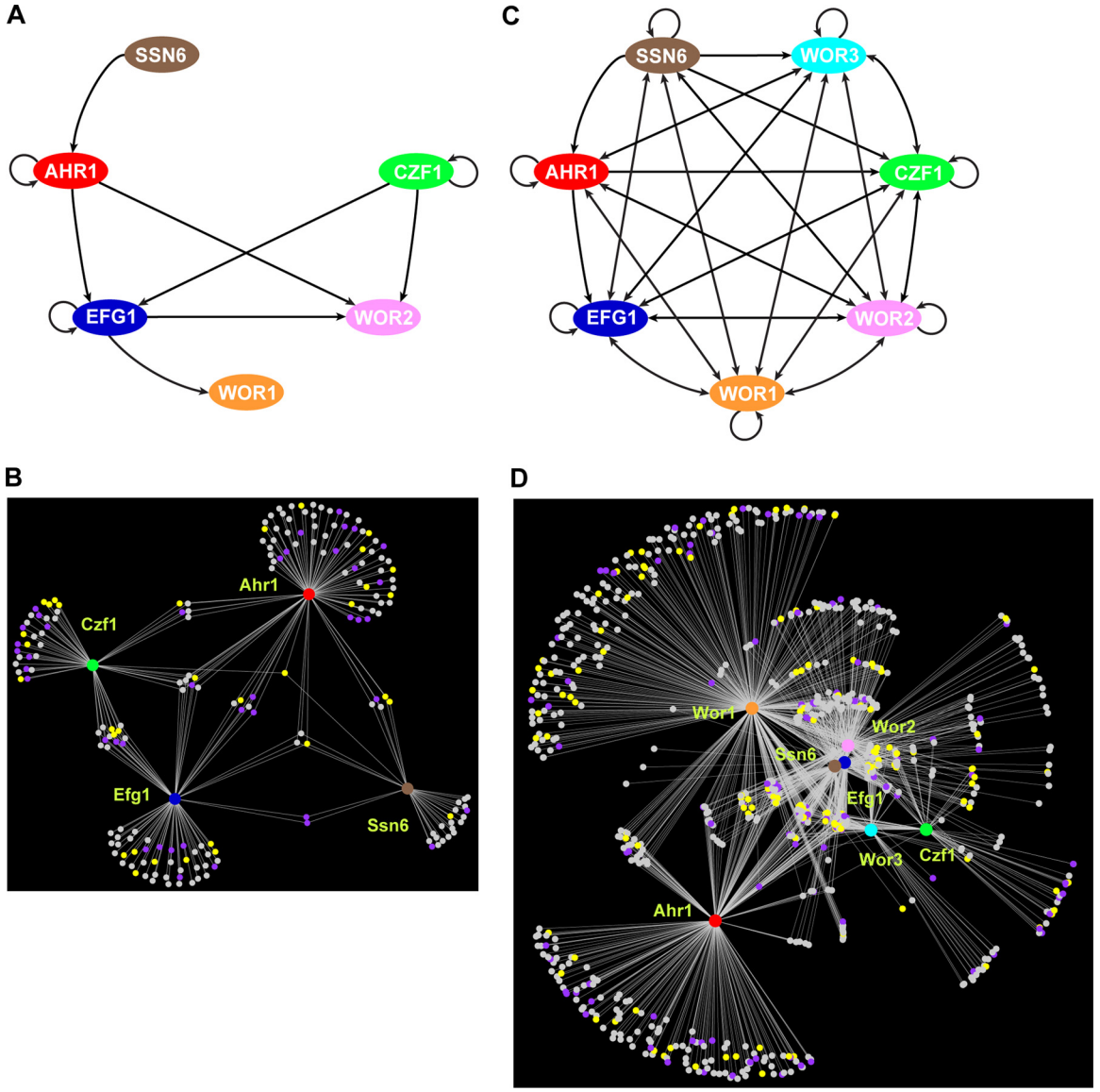

FIG 4 The white and opaque cell regulatory networks as determined by ChIP-chip analysis. The core regulatory networks in white (a) and opaque (c) cells as well as the full white (b) and opaque (d) regulatory networks are shown. The white cell network consists of four core regulators (Ahr1, red; Czf1, green; Efg1, blue; Ssn6, brown), while the opaque cell network consists of three additional regulators (Wor1, orange; Wor2, pink; Wor3, light blue), for a total of seven regulators. (a and c) The white cell (a) and opaque cell (c) core regulatory networks. Arrows represent direct binding interactions for the various transcriptional regulators. (b and d) The full white cell (b) and opaque cell (d) regulatory networks. The core regulators are represented by the large circular hubs, while target genes are represented by the smaller circles. Target genes are connected to their respective regulators by white lines, indicative of a direct binding interaction assessed by ChIP-chip analysis. Genes differentially regulated as determined by RNA-seq performed by Tuch et al. (26) in opaque compared to white cells are shown in yellow for genes upregulated in opaque cells, in light purple for genes downregulated in opaque cells, and in gray for genes with no change. ChIP-chip data are taken from the present study as well as from several previous studies (17, 23, 24).

from such a result, a search for DNA sequences overrepresented in the Ssn6 binding sites produced the canonical Wor1 motif (WTTWARSTTT) (24, 31) (see Fig. S3C and D). However, the rules of Ssn6 recruitment cannot be as simple as the requirement of the presence of Wor1, Wor2, and/or Efg1, as there are many sites in the genome bound by one or both of these regulators that are not enriched for Ssn6 binding. As has been established in *S. cerevisiae*, numerous combinations of regulatory proteins can recruit Ssn6 to sites on DNA; for *C. albicans*, the precise "rules" of recruitment remain to be worked out, although we know that Wor1, Wor2, and Efg1 are key players.

DISCUSSION

The regulatory network controlling white-opaque switching in *C. albicans* is large, complex, and highly interconnected. Three properties of the network suggest rationales for this complexity. (i) The circuit exhibits an extreme example of bimodality, with each state being stable for ~10^4 cell generations. (ii) The circuit controls the expression of about 20% of the protein coding genes in the *C. albicans*

genome. (iii) The extent to which genes are white- or opaque-phase-enriched varies enormously from one gene to the next: some are tightly shut off in one of the two cell types, but most exhibit more graded expression differences. In this paper, we demonstrate that the Ssn6 transcriptional corepressor is a key regulator of the white-opaque circuit. Ssn6 is critical for the stability of the white cell type and also plays a widespread role in the regulation of both the white and the opaque cell transcriptional programs.

The characterization of Ssn6's role in the white-opaque regulatory network requires a refinement to our current conception of how switching between the two cell types is regulated. In a wild-type strain, under normal laboratory conditions, switching to the opaque cell type occurs in a stochastic manner. When either *EFG1* or *AHR1* is deleted from **a** or α cells, the switch to the opaque cell type still occurs randomly, although at a significantly higher frequency than in wild-type **a** or α cells. Deletion of *SSN6*, however, results in immediate and complete switching to the opaque cell type as long as an intact *WOR1* gene is present. This deterministic, as opposed to stochastic, nature of switching in the *ssn6* deletion mutant indicates that white cells actively repress the machinery needed to trigger the switch to the opaque cell type, with Ssn6 at the center of this repression. In other words, Ssn6 is necessary for the stochastic nature of the switch.

In addition to maintaining the stochastic properties of white-to-opaque switching, Ssn6 also plays a role in the proper expression of the transcriptional program specific to both white and opaque cells. Ssn6 is required to prevent activation of the opaque cell specification program in white cells; however, the majority of that regulatory control is exerted indirectly through the maintenance of low-level *WOR1* expression. In other words, Ssn6 does not directly repress the entire opaque cell transcriptional program in white cells but, rather, prevents excitation of the transcriptional circuit that leads to elevated *WOR1* expression and transition to the opaque state. As discussed above, there are a few opaque-phase-specific genes whose expression is directly repressed by Ssn6, independently of Wor1.

The role of Ssn6 expands in opaque cells, as it occupies many more regions of the genome and appears to be recruited largely by the opaque-phenotype-specific "master" transcriptional regulators, most prevalently Wor1 and Wor2. Thus, in opaque cells, Ssn6 is important for the specification of the opaque cell phenotype and is required for the repression of the majority of the white cell transcriptional program. In addition to these cell type-specific roles, Ssn6 also is important for the repression of a number of other genes whose expression is not enriched in either cell type (Fig. 5).

The work in this paper adds another layer of complexity to the regulation of white-opaque switching in *C. albicans*. Previous analysis concentrated on a group of sequence-specific DNA binding proteins that underlie the switch, and the current work shows that Ssn6, recruited by certain combinations of these proteins, is equally important to the switch. In particular, when *SSN6* is deleted, cells are tightly locked in the opaque cell type and the stochastic nature of the switch is lost. Although it appears to act as a general repressor, regulating many genes of diverse functions (including those that have little, if any, relation to the white-opaque switch), there is a dramatic shift in the distribution of Ssn6 across the genome when cells switch from the white cell type to the opaque cell type. Our work indicates that this shift is crucial both for the specification of the two distinctive cell types and for controlling the frequency of switching between them.

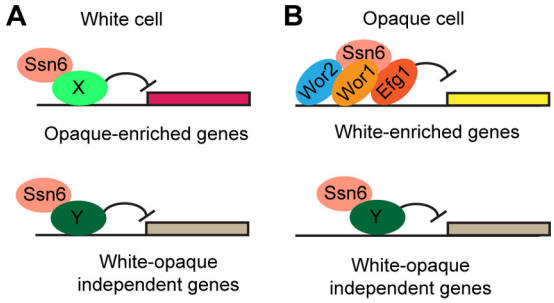

FIG 5 Model of a subset of Ssn6 repression in the white and opaque cell types. (a) In white a/a cells, some opaque-phase-enriched genes are directly or indirectly repressed by Ssn6 independently of Wor1 (top) in coordination with an undetermined "X" cofactor. (b) In opaque a/a cells, a majority of white-phase-enriched genes are directly or indirectly repressed by Ssn6, possibly in combination with Wor1, Wor2, and/or Efg1 (top). In both cell types, Ssn6 represses a number of genes that are neither white enriched nor opaque enriched (bottom). Arrows and bars represent activation and repression, respectively, and reflect both direct and indirect regulation.

MATERIALS AND METHODS

Growth conditions. All strains were grown on synthetic complete media supplemented with 2% glucose and 100 μg/ml uridine (SD + aa + uri) at room temperature unless otherwise noted. Both white and opaque cell cultures for ChIP-chip or expression microarray experiments were assessed by microscopy to ensure a homogenous cell population.

Plasmid construction. A list of plasmids used in this study can be found in Data Set S4A in the supplemental material. A list of oligonucleotides used in this study can be found in Data Set S4B. Plasmids for deleting one copy of the mating type locus (pJD1 [32]), the recyclable *SAT1* (nourseothricin resistance [NAT^r]) flipper system (pSFS2a [33]), and N-terminal 7× Myc epitope tagging of a gene (pADH70 [34]) have been previously reported.

The *SSN6* ectopic expression construct was generated by cloning the *SSN6* open reading frame (ORF) with BglII and XmaI restriction sites at the 5′ and 3′ ends, respectively. This fragment was then cloned into the BamHI and XmaI restriction sites in the previously reported pADH33 p*MET3-SAT1* vector (17) to generate plasmid pADH58. Unmodified pADH33 served as an empty vector control for pADH58.

Plasmid pADH109, containing a nourseothricin resistance cassette flanked by 500 bp of genomic DNA sequence from either side of the *C. albicans* MTL locus, was assembled *in vitro* via circular polymerase extension cloning (35). Fragment 1 contained an *Escherichia coli* plasmid backbone plus the *MTL* flanking sequence amplified from pJD1 (31) with AHO1001 and AHO1002. Fragment 2 contained the *C. albicans* NAT^r cassette amplified from pSFS2a (32) using AHO997 and AHO1003. Oligonucleotide sequences are included in Data Set S4B in the supplemental material.

Strain construction. A list of strains used in this study can be found in Data Set S4C in the supplemental material. The initial white-opaque switching-capable *ssn6* deletion strains were generated by converting a/α *ssn6* deletion strain TF121 (27) to a/Δ and α/Δ using the pJD1 mating type locus knockout vector (32).

An independent *ssn6* deletion mutant strain was generated using a previously reported sorbose-selected a/a strain (RZY47 [21]) as previously described (36). Briefly, DNA sequences flanking the *SSN6* ORF were amplified, fused to either the *HIS1* or *LEU2* marker by stitching PCR, and transformed into RZY47. Correct chromosomal integration and orientation of each marker were verified by colony PCR, as was the loss of the *SSN6* ORF.

In order to construct the *ssn6 wor1* double-deletion mutant strain, we first made a new *wor1* deletion strain using the recyclable *SAT1* flipper system (33). Using primers with homology to the flanks of the *WOR1* ORF, we amplified the *SAT1*-flp cassette from pSFS2a (33). We then transformed this strain into the RZY47 background, verified proper integration through colony PCR, recycled the *SAT1* marker, and repeated the transformation to knock out the second copy of *WOR1*. Deletion of *WOR1* was confirmed via colony PCR, and the *SAT1* marker was again removed. We then deleted both copies of *SSN6* as described above.

The a/Δ *tup1* deletion strain was generated by converting a/α *tup1* deletion strain TF117 (27) to a/Δ using the pJD1 mating type locus knockout vector (32).

The empty vector control strains for the ectopic overexpression experiments have been previously reported (17). The *SSN6* ectopic expression strains were generated by integrating linearized pADH58 (*SSN6*) at the RP10 (*RPS1*) locus. Correct integration and orientation of the expression construct were verified by colony PCR.

N-terminal epitope tagging of Ssn6 with 7× Myc was performed using pADH70 (34) as previously described (37).

Nourseothricin-resistant arg-negative (arg$^-$) *MTLa* strains (AHY604 and AHY611) were created by replacing the *MTLα* locus with a NAT^r-marked integration cassette (contained within plasmid pADH109). *MTLα* knockouts were confirmed by colony PCR with the following primer pairs: *MTLa*-specific primers AHO983 and AHO987 and *MTLα*-specific primers AHO985 and AHO986 (see Data Set S4B in the supplemental material for oligonucleotide sequences). AHY613 was derived from AHY604 by spontaneous white-to-opaque switching.

Switching assays. Plate-based quantitative white-opaque switching and ectopic expression assays were performed as previously described (7, 23). For the quantitative white-opaque switching assay, strains were grown for 1 week at room temperature. Five entirely white or opaque colonies were resuspended in water, diluted, plated on SD + aa + uri, allowed to grow for 1 week at room temperature, and scored for switching events (both colonies of the starting cell type with one or more sectors of the other cell type and colonies fully of the other cell type). Due to the altered colony phenotypes exhibited by the strain with the *ssn6* deletion in the a/α background, we examined cells from representative colonies under a microscope prior to scoring plates in order to properly match the colony with the single-cell morphology. It was not possible to perform a standard quantitative white-to-opaque switching assay for the a/a *ssn6*, a/Δ *ssn6*, and α/Δ *ssn6* deletions due to the locked opaque nature of these strains.

Strains for ectopic expression assays were grown for 1 week on repressing media (Met$^+$ Cys$^+$). Five entirely white or opaque colonies were resuspended in water, diluted, and then plated on either repressing or inducing (Met$^-$ Cys$^-$) media, allowed to grow for 7 days at room temperature, and scored with the empty vector strains used as negative controls.

Cell microscopy images were taken from overnight cultures (SD + aa + uri at room temperature) started from representative colonies. Microscopic images were taken using a Zeiss Axiovert 200M microscope.

Mating assays. Quantitative mating assays were performed using the *MTLa* and *MTLα* mating pairs indicated in Table S2 in the supplemental material. All strains were grown on SD plus amino acid (SD + aa) agar plates at 25°C for 7 days to isolate white or opaque colonies. Two independent single colonies were selected for each strain, inoculated into SD + aa liquid media, and cultured overnight at 25°C with orbital shaking. Overnight cultures were diluted to an optical density (OD) of 0.2 and cultured at 25°C with shaking until the OD reached 0.5. For each mating cross, ~2×10^7 cells of the "tester" strain were mixed with ~4×10^6 cells of the limiting "donor" strain. Mating mixtures were pelleted by centrifugation at 6,000 × *g* for 2 min, resuspended in 20 μl of SD + aa media, spotted onto Spider medium plates, and incubated at 25°C for 48 h. The samples from each mating mixture were then recovered with a sterile applicator stick, resuspended in 1 ml SD without amino acids (SD−aa), and homogenized 5 times for 1 min each time in a Bransonic M3800 bath sonicator. After normalizing each mating mixture to ~2×10^7 cells per ml, 1 ml of each mating mixture was pelleted by centrifugation (2 min at 10,000 × *g*) and then washed, resuspended, and diluted serially in SD − aa media. Dilutions were plated on SD without arginine (arg) and with nourseothricin (300 μg/ml) to select for mating products and plated on SD-arginine to select for the mating products plus the limiting parent. Plates were cultured for 3 days at 30°C and scored for colony growth. Mating frequency was calculated as follows: mating frequency = [number of mating products (SD − arg + NAT)]/[(number of mating products + number of limiting parents (SD − arg)].

Microarrays. Three independent microarray experiments were performed for each strain. One replicate (replicate C) used cells grown to mid-log phase in SD + aa + uri at 25°C. The other two replicates (replicates A and B) used cells grown under identical conditions but with arginine supplemented into the growth media at a concentration of 2.5 mg/ml to accommodate a growth defect likely associated with the arg$^-$ genotype of our a/α strains. RNA isolation and cDNA synthesis were performed as previously described (38). A pooled reference was made using equal proportions of aa-cDNA from each strain to be hybridized on the array. The pooled reference was labeled with Cy3, and the experimental strains were all labeled with Cy5. Equal amounts of Cy3-labeled and Cy5-labeled samples were hybridized to 8x15K microarrays (AMADID no. 020166), and arrays were scanned using a GenePix 4000B microarray scanner. Array images were gridded using GenePix Pro version 7, and global LOWESS normalization was performed for each array using a Goulphar script written for R (39). Normalized data for independent probes corresponding to the same ORF was then collapsed using a Python script. Processed, transformed data for key comparisons can be found in Data Set S1 in the supplemental material.

The three repeats for each strain were divided into three groups (groups A, B, and C), keeping replicates processed on a given day together. There was an extra replicate of the a/a *ssn6* deletion in each group, giving six total repeats for this genotype. Transformations (i.e., a/a opaque versus a/a white) were performed within each group (i.e., a/a opaque A versus a/a white A, a/a opaque B versus a/a white B, and so on), with the three extra a/a *ssn6* deletion replicates also transformed against the same strains that the first copy was transformed against (i.e., a/a *ssn6* deletion A and a/a *ssn6* deletion repeat A versus a/a white A).

Lists of genes meeting specific criteria (i.e., enriched by at least 3-fold in a deletion strain relative to the wild type) were developed as follows. Whether three or six replicates were available, we required that the median value exceed the given threshold. The number of genes changing in a given deletion strain excludes the gene or genes that were deleted in that case (i.e., *SSN6* in an *ssn6* deletion strain). Lists of white-phase-enriched and opaque-phase-enriched genes are based on the data from this transcriptional analysis as well as on previously reported RNAseq data (26). In addition, we created a high-confidence set of genes that were white or opaque phase enriched 2- or 3-fold in each of four different experiments (24, 26, 30; this study). Figure 3 and Fig. S2 in the supplemental material show the median value for each set of transformations.

ChIP-chip analysis. Cultures for chromatin immunoprecipitation were harvested during mid-log phase by centrifugation. Chromatin immunoprecipitation, strand displacement amplification, dye coupling, and hybridization to a custom 1x244K Agilent tiling microarray (AMADID no. 016350) were performed as described previously (34, 37). We used two custom antibodies against Ssn6 as well as an anti-Myc monoclonal antibody (Invitrogen AHO0062) for N-terminally Myc-tagged Ssn6. Ssn6 custom antibodies were raised against the sequences CPPAKPHGAPQQRTG (residues 664 to 677; referred to here as anti-664) and CETKKDTTKTSPAKQ (residues 1005 to 1018; referred to here as anti-1005) (GenScript). Full-genome ChIP-chip experiments on Ssn6 in white cells used anti-664 antibodies and were performed twice. Full-genome ChIP-chip experiments on Ssn6 in opaque cells were performed once with each custom antibody and once with anti-Myc for the 7× Myc-Ssn6 strain.

Arrays were scanned using a Genepix 4000B scanner (Axon Instruments/Molecular Devices) and processed as described previously (34) with the following exception: minimum enrichment cutoffs for MochiView (40) peak detection were set to the default 0.58 value for the tagged/wild-type arrays and to 0.27 for the untagged/deletion arrays. Peak sizes were set to 500 bp. These settings are identical to those previously used for the analysis of Wor1, Wor2, Wor3, Czf1, Efg1, and Ahr1 binding (17, 24). Peaks were then filtered by the subtraction of a previously reported set of likely artifactual peaks which show variable but substantial enrichment in many control ChIP-chip experiments performed using antibodies against a deleted target (17, 24).

For the white cell Ssn6 ChIP-chip experiments, two independent experiments were performed with anti-664 against a wild-type a/a white strain and two independent control experiments were performed against an a/a strain deleted for *ssn6*. The two experimental and control experiments were merged and the peaks then identified by MochiView using the settings described above. One peak was manually added (upstream of orf19.1906 and orf19.1907) based on a manual examination of the data.

For the opaque cell Ssn6 ChIP-chip experiments, the processed peak calls from the three independent experiments (262 in anti-Myc, 91 in anti-664, and 178 in anti-1005) were then further processed as follows. Any binding sites in the Myc data set that overlapped a peak from either of the custom antibodies (176 peaks) were taken, and the location was defined based on that of the Myc data set. Peaks in the Myc data set that did not directly overlap a custom antibody peak but that were part of the flanking enriched area of a broader custom antibody peak (47 sites) were also taken. A further 5 Myc data set sites that did not follow these criteria were also taken on the basis of visual inspection of all datasets at that location. A further 9 locations that were not called in the Myc data set but that were called in both custom antibody datasets were also taken; the anti-1005 data set locations and enrichment were used for these peaks. This resulted in a total of 237 peaks of size 500 bp which we used for all subsequent analysis. The analyzed ChIP-chip data are included in Data Set S1 in the supplemental material. Plots of the areas of peak enrichment for Ssn6 in both cell types are included in Data Set S2.

Subsequent analysis of the ChIP-chip binding sets (binding overlap determination, calculation of the number of events observed versus number expected) was performed using MochiView as previously described (17, 24). The list of transcriptional regulators is based on Dataset S1 in the supplemental material provided by Homann et al. (27) as modified in Hernday et al. (24). Binding sites for the other six regulators of white-opaque switching were taken from the ChIP-chip datasets previously reported (17, 23, 24).

Accession numbers. Raw gene expression array data determined in this work are available at the Gene Expression Omnibus (GEO) (http://www.ncbi.nlm.nih.gov/geo; accession no. GSE74011). Raw ChIP-chip data are also available at GEO (accession no. GSE58054).

SUPPLEMENTAL MATERIAL

Supplemental material for this article may be found at http://mbio.asm.org/lookup/suppl/doi:10.1128/mBio.01565-15/-/DCSupplemental.

Figure S1, TIF file, 0.7 MB.
Figure S2, TIF file, 0.7 MB.
Figure S3, TIF file, 0.5 MB.
Table S1, DOCX file, 0.02 MB.
Table S2, DOCX file, 0.01 MB.
Table S3, DOCX file, 0.01 MB.
Data Set S1, XLSX file, 1.4 MB.
Data Set S2, PDF file, 2.1 MB.
Data Set S3, XLSX file, 0.03 MB.
Data Set S4, XLSX file, 0.02 MB.

ACKNOWLEDGMENTS

We are grateful to Oliver Homann for developing MochiView and to Victor Hanson-Smith for creating a Python script to assist in microarray data analysis. We thank Ananda Mendoza and Glenda Polack for technical assistance.

This study was supported by NIH grants R01AI049187 (A.D.J.), F32AI071433 (A.D.H.), and R00AI100896 (C.J.N.).

The content is the sole responsibility of the authors and does not represent the views of the NIH.

A.D.J. and C.J.N. are cofounders of BioSynesis, Inc., a company developing inhibitors and diagnostics of *C. albicans* biofilm formation, and M.B.L. is an employee of BioSynesis, Inc.; however, we have no conflicts of interest to declare with regard to the manuscript.

FUNDING INFORMATION

HHS | NIH | National Institute of Allergy and Infectious Diseases (NIAID) provided funding to ALEXANDER D JOHNSON under grant number R01AI049187. HHS | NIH | National Institute of Allergy and Infectious Diseases (NIAID) provided funding to Clarissa J Nobile under grant number R00AI100896. HHS | NIH | National Institute of Allergy and Infectious Diseases (NIAID) provided funding to Aaron D Hernday under grant number F32AI071433.

REFERENCES

1. **Johnson A**. 2003. The biology of mating in Candida albicans. Nat Rev Microbiol **1:**106–116. http://dx.doi.org/10.1038/nrmicro752.
2. **Lohse MB, Johnson AD**. 2009. White-opaque switching in Candida albicans. Curr Opin Microbiol **12:**650–654. http://dx.doi.org/10.1016/j.mib.2009.09.010.
3. **Morschhäuser J**. 2010. Regulation of white-opaque switching in Candida albicans. Med Microbiol Immunol **199:**165–172. http://dx.doi.org/10.1007/s00430-010-0147-0.
4. **Slutsky B, Staebell M, Anderson J, Risen L, Pfaller M, Soll DR**. 1987. "White-opaque transition": a second high-frequency switching system in *Candida albicans*. J Bacteriol **169:**189–197.
5. **Soll DR**. 2009. Why does Candida albicans switch? FEMS Yeast Res **9:**973–989. http://dx.doi.org/10.1111/j.1567-1364.2009.00562.x.
6. **Soll DR, Morrow B, Srikantha T**. 1993. High-frequency phenotypic switching in Candida albicans. Trends Genet **9:**61–65. http://dx.doi.org/10.1016/0168-9525(93)90189-O.
7. **Miller MG, Johnson AD**. 2002. White-opaque switching in Candida albicans is controlled by mating-type locus homeodomain proteins and allows efficient mating. Cell **110:**293–302. http://dx.doi.org/10.1016/S0092-8674(02)00837-1.
8. **Lan CY, Newport G, Murillo LA, Jones T, Scherer S, Davis RW, Agabian N**. 2002. Metabolic specialization associated with phenotypic switching in Candida albicans. Proc Natl Acad Sci U S A **99:**14907–14912. http://dx.doi.org/10.1073/pnas.232566499.
9. **Geiger J, Wessels D, Lockhart SR, Soll DR**. 2004. Release of a potent polymorphonuclear leukocyte chemoattractant is regulated by white-opaque switching in Candida albicans. Infect Immun **72:**667–677. http://dx.doi.org/10.1128/IAI.72.2.667-677.2004.
10. **Kvaal CA, Srikantha T, Soll DR**. 1997. Misexpression of the white-phase-specific gene WH11 in the opaque phase of Candida albicans affects switching and virulence. Infect Immun **65:**4468–4475.
11. **Lohse MB, Johnson AD**. 2008. Differential phagocytosis of white versus opaque Candida albicans by drosophila and mouse phagocytes. PLoS One **3:**e1473. http://dx.doi.org/10.1371/journal.pone.0001473.
12. **Kvaal C, Lachke SA, Srikantha T, Daniels K, McCoy J, Soll DR**. 1999. Misexpression of the opaque-phase-specific gene PEP1 (SAP1) in the white phase of Candida albicans confers increased virulence in a mouse model of cutaneous infection. Infect Immun **67:**6652–6662.
13. **Sasse C, Hasenberg M, Weyler M, Gunzer M, Morschhäuser J**. 2013. White-opaque switching of Candida albicans allows immune evasion in an environment-dependent fashion. Eukaryot Cell **12:**50–58. http://dx.doi.org/10.1128/EC.00266-12.
14. **Rikkerink EH, Magee BB, Magee PT**. 1988. Opaque-white phenotype transition: a programmed morphological transition in Candida albicans. J Bacteriol **170:**895–899.
15. **Huang G, Srikantha T, Sahni N, Yi S, Soll DR**. 2009. CO(2) regulates white-to-opaque switching in Candida albicans. Curr Biol **19:**330–334. http://dx.doi.org/10.1016/j.cub.2009.01.018.
16. **Huang G, Yi S, Sahni N, Daniels KJ, Srikantha T, Soll DR**. 2010.

N-acetylglucosamine induces white to opaque switching, a mating prerequisite in Candida albicans. PLoS Pathog **6:**e1000806. http://dx.doi.org/10.1371/journal.ppat.1000806.

17. **Lohse MB, Hernday AD, Fordyce PM, Noiman L, Sorrells TR, Hanson-Smith V, Nobile CJ, DeRisi JL, Johnson AD.** 2013. Identification and characterization of a previously undescribed family of sequence-specific DNA-binding domains. Proc Natl Acad Sci U S A **110:**7660–7665. http://dx.doi.org/10.1073/pnas.1221734110.
18. **Huang G, Wang H, Chou S, Nie X, Chen J, Liu H.** 2006. Bistable expression of WOR1, a master regulator of white-opaque switching in Candida albicans. Proc Natl Acad Sci U S A **103:**12813–12818. http://dx.doi.org/10.1073/pnas.0605270103.
19. **Srikantha T, Borneman AR, Daniels KJ, Pujol C, Wu W, Seringhaus MR, Gerstein M, Yi S, Snyder M, Soll DR.** 2006. TOS9 regulates white-opaque switching in Candida albicans. Eukaryot Cell **5:**1674–1687. http://dx.doi.org/10.1128/EC.00252-06.
20. **Wang H, Song W, Huang G, Zhou Z, Ding Y, Chen J.** 2011. Candida albicans Zcf37, a zinc finger protein, is required for stabilization of the white state. FEBS Lett **585:**797–802. http://dx.doi.org/10.1016/j.febslet.2011.02.005.
21. **Zordan RE, Galgoczy DJ, Johnson AD.** 2006. Epigenetic properties of white-opaque switching in Candida albicans are based on a self-sustaining transcriptional feedback loop. Proc Natl Acad Sci U S A **103:**12807–12812. http://dx.doi.org/10.1073/pnas.0605138103.
22. **Vinces MD, Kumamoto CA.** 2007. The morphogenetic regulator Czf1p is a DNA-binding protein that regulates white opaque switching in Candida albicans. Microbiology **153:**2877–2884. http://dx.doi.org/10.1099/mic.0.2007/005983-0.
23. **Zordan RE, Miller MG, Galgoczy DJ, Tuch BB, Johnson AD.** 2007. Interlocking transcriptional feedback loops control white-opaque switching in Candida albicans. PLoS Biol **5:**e256. http://dx.doi.org/10.1371/journal.pbio.0050256.
24. **Hernday AD, Lohse MB, Fordyce PM, Nobile CJ, DeRisi JL, Johnson AD.** 2013. Structure of the transcriptional network controlling white-opaque switching in Candida albicans. Mol Microbiol **90:**22–35. http://dx.doi.org/10.1111/mmi.12329.
25. **Sonneborn A, Tebarth B, Ernst JF.** 1999. Control of white-opaque phenotypic switching in Candida albicans by the Efg1p morphogenetic regulator. Infect Immun **67:**4655–4660.
26. **Tuch BB, Mitrovich QM, Homann OR, Hernday AD, Monighetti CK, De La Vega FM, Johnson AD.** 2010. The transcriptomes of two heritable cell types illuminate the circuit governing their differentiation. PLoS Genet **6:**e1001070. http://dx.doi.org/10.1371/journal.pgen.1001070.
27. **Homann OR, Dea J, Noble SM, Johnson AD.** 2009. A phenotypic profile of the Candida albicans regulatory network. PLoS Genet **5:**e1000783. http://dx.doi.org/10.1371/journal.pgen.1000783.
28. **García-Sánchez S, Mavor AL, Russell CL, Argimon S, Dennison P, Enjalbert B, Brown AJ.** 2005. Global roles of Ssn6 in Tup1- and Nrg1-dependent gene regulation in the fungal pathogen, Candida albicans. Mol Biol Cell **16:**2913–2925. http://dx.doi.org/10.1091/mbc.E05-01-0071.
29. **Park YN, Morschhäuser J.** 2005. Candida albicans MTLalpha tup1Delta mutants can reversibly switch to mating-competent, filamentous growth forms. Mol Microbiol **58:**1288–1302. http://dx.doi.org/10.1111/j.1365-2958.2005.04898.x.
30. **Lohse MB, Johnson AD.** 2010. Temporal anatomy of an epigenetic switch in cell programming: the white-opaque transition of C. albicans. Mol Microbiol **78:**331–343. http://dx.doi.org/10.1111/j.1365-2958.2010.07331.x.
31. **Lohse MB, Zordan RE, Cain CW, Johnson AD.** 2010. Distinct class of DNA-binding domains is exemplified by a master regulator of phenotypic switching in Candida albicans. Proc Natl Acad Sci U S A **107:**14105–14110. http://dx.doi.org/10.1073/pnas.1005911107.
32. **Lin CH, Kabrawala S, Fox EP, Nobile CJ, Johnson AD, Bennett RJ.** 2013. Genetic control of conventional and pheromone-stimulated biofilm formation in Candida albicans. PLoS Pathog **9:**e1003305. http://dx.doi.org/10.1371/journal.ppat.1003305.
33. **Reuss O, Vik A, Kolter R, Morschhäuser J.** 2004. The SAT1 flipper, an optimized tool for gene disruption in Candida albicans. Gene **341:**119–127. http://dx.doi.org/10.1016/j.gene.2004.06.021.
34. **Nobile CJ, Fox EP, Nett JE, Sorrells TR, Mitrovich QM, Hernday AD, Tuch BB, Andes DR, Johnson AD.** 2012. A recently evolved transcriptional network controls biofilm development in Candida albicans. Cell **148:**126–138. http://dx.doi.org/10.1016/j.cell.2011.10.048.
35. **Quan J, Tian J.** 2009. Circular polymerase extension cloning of complex gene libraries and pathways. PLoS One **4:**e6441. http://dx.doi.org/10.1371/journal.pone.0006441.
36. **Noble SM, Johnson AD.** 2005. Strains and strategies for large-scale gene deletion studies of the diploid human fungal pathogen Candida albicans. Eukaryot Cell **4:**298–309. http://dx.doi.org/10.1128/EC.4.2.298-309.2005.
37. **Hernday AD, Noble SM, Mitrovich QM, Johnson AD.** 2010. Genetics and molecular biology in Candida albicans. Methods Enzymol **470:**737–758. http://dx.doi.org/10.1016/S0076-6879(10)70031-8.
38. **Nobile CJ, Nett JE, Hernday AD, Homann OR, Deneault JS, Nantel A, Andes DR, Johnson AD, Mitchell AP.** 2009. Biofilm matrix regulation by Candida albicans Zap1. PLoS Biol **7:**e1000133. http://dx.doi.org/10.1371/journal.pbio.1000133.
39. **Lemoine S, Combes F, Servant N, Le Crom S.** 2006. Goulphar: rapid access and expertise for standard two-color microarray normalization methods. BMC Bioinformatics **7:**467. http://dx.doi.org/10.1186/1471-2105-7-467.
40. **Homann OR, Johnson AD.** 2010. MochiView: versatile software for genome browsing and DNA motif analysis. BMC Biol **8:**49. http://dx.doi.org/10.1186/1741-7007-8-49.